# Impedance Transformation and Matching for Lumped Complex Load with Nonuniform Transmission Line

ISAO ENDO, YOSHIAKI NEMOTO, MEMBER, IEEE, AND RISABURO SATO, FELLOW, IEEE

*Abstract*—**New nonuniform transmission-line matching networks for a class of lumped complex loads are presented. A parabolic (or reciprocal parabolic) tapered transmission line, whose exact equivalent circuit is represented by a mixed lumped and distributed circuit, can transform the lumped series *RC* (or parallel *RL*) loads into different lumped impedances which are more convenient than the original load impedances for ordinary matching network design. Simple design procedures are described and useful design charts are given. Also, numerical examples are shown including experimental verification.**

## I. Introduction

An important and interesting problem in microwave engineering is the design of impedance matching networks for complex loads. A number of design methods have been previously investigated and applied to microwave circuits [1], [2].

Designs for matching networks may be classified into several categories according to their purposes and operation, namely, the matching network 1) designed as a one-point matching or broad-band equalizer, 2) designed for a complex or real load, 3) constructed with lumped elements or distributed ones, etc. [3]–[7].

In this paper, we propose a new approach to solve a complex matching problem using nonuniform transmission lines for lumped complex loads. It is well known that nonuniform transmission lines show superior responses to those of uniform transmission lines, but it is difficult to find the exact network functions of general nonuniform transmission lines from the telegrapher's equation except for special cases [8]–[12]. On the other hand, we have shown a new method to obtain an exact network function of a class of nonuniform transmission lines based on new equivalent transformations [13], [14]. In the case of the parabolic tapered transmission line (PTL), its equivalent circuit is given as the circuit consisting of a cascade connection of a lumped capacitor, a uniform transmission line, a negative lumped capacitor, and an ideal transformer [13]. The equivalent circuit of the reciprocal parabolic tapered transmission line (RPTL) is given as the dual circuit of the PTL circuit. By attending to the negative lumped elements appearing in these equivalent circuits, we can discuss the nonuniform transmission-line impedance transformation and matching network for lumped complex loads. Both the PTL and RPTL may transform the lumped load impedance into different lumped impedances which are more convenient than the original load impedance for an ordinary matching network design. When the real part of a lumped series *RC* load is larger than the reference impedance, the PTL may decrease the level of the original load impedance in all frequency ranges. A quarter-wavelength PTL may transform any lumped series *RC* load into another convenient driving point impedance in narrow frequency ranges. The RPTL impedance transformation network can be treated as the dual of the PTL. We also demonstrate the usefulness of these procedures of impedance transformation and matching by numerical examples, including experimental verification.

Manuscript received March 19, 1984; revised July 20, 1984.

I. Endo is with the Department of Electrical Engineering, Ibaraki Technical College, Katsuta 312, Japan.

Y. Nemoto and R. Sato are with the Department of Information Science, Faculty of Engineering, Tohoku University, Sendai 980, Japan.

## II. Impedance Transformation and Matching for Lumped *RC* Loads with Parabolic Tapered Transmission Lines

A PTL, whose characteristic impedance distribution is given by

$$W(x) = W_0\left(1+\frac{1x}{K_2 l}\right)^2 \tag{1}$$

is represented by a mixed lumped and distributed equivalent circuit as shown in Fig. 1, where $W_0$ is the front-end ($x = 0$) characteristic impedance, $K_1$ is a positive constant, and $l$ is a line length of the PTL. In the equivalent circuit, the element values are given as follows [13]:

$$k = 1+\frac{1}{K_1} > 1 \tag{2}$$

$$\mathbb{W}_0 = k^2 W_0 \tag{3}$$

$$\mathbb{C}_0 = (1+K_1) l/\left(k^2 W_0 \nu\right) \tag{4}$$

and $\nu$ denotes the velocity of light. Note that the lumped capacitor located at the right-hand side of the equivalent circuit is a negative one.

The PTL loaded by lumped series *RC* impedance of $Z_L$

$$Z_L = R_L + \frac{1}{j\omega C_L} \tag{5}$$

is shown in Fig. 2(a) and its equivalent circuit is shown in Fig. 2(b).

0018-9480/85/0100-0002$01.00 ©1984 IEEE

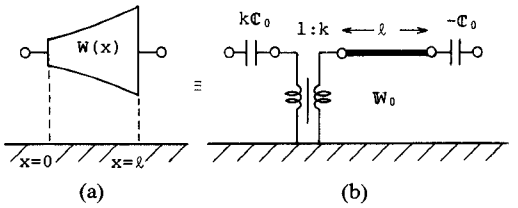


Fig. 1. (a) The parabolic tapered transmission line and (b) its equivalent circuits.

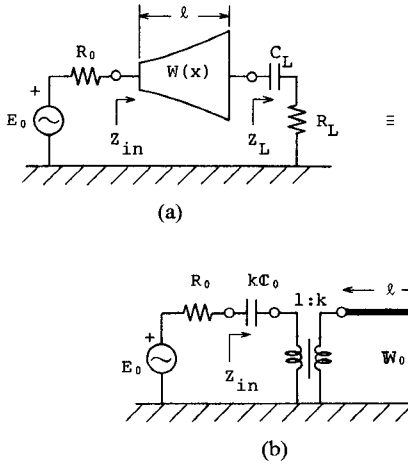


Fig. 2. (a) The parabolic tapered transmission line loaded by lumped series $RC$ impedance and (b) its equivalent circuit.

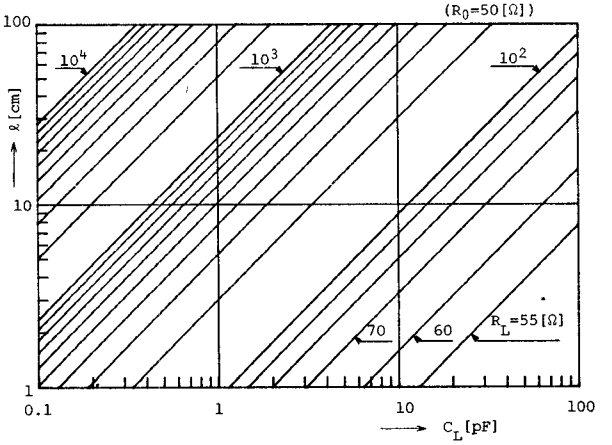


Fig. 3. The line length $l$ versus $C_L$ for $R_0 = 50\ \Omega$.

TABLE I
THE PARAMETERS OF PTL'S FOR NUMERICAL EXAMPLES OF ALL-FREQUENCY TRANSFORMATION

| $Z_L$ | | k | $W_0$[Ω] | $K_1$ | ℓ[cm] |
|---|---|---|---|---|---|
| load A | $R_L$ = 500[Ω], $C_L$ = 2[pF] | 3.16 | 50 | 0.462 | 20.5 |
| load B | $R_L$ = 300[Ω], $C_L$ = 2[pF] | 2.45 | 50 | 0.690 | 10.7 |

In Fig. 2(b), the negative capacitor $-\mathbb{C}_0$ in the equivalent circuit of the PTL may cancel out the capacitor $C_L$ in the complex load when $\mathbb{C}_0$ equals $C_L$. By choosing appropriate values for the characteristic impedance $\mathbb{W}_0$ and the line length $l$ of the uniform transmission line and the transformation ratio $k$ of the ideal transformer (IT), the driving point impedance $Z_{in}$ becomes a lumped series $RC$ impedance, which is, in general, different from the load impedance $Z_L$.

### A. Impedance Transformation for all Frequency Ranges

Procedures of impedance transformation for all frequency ranges are summarized in the following four steps, where we assume that the reference impedance is $R_0\ \Omega$.

Step 1) Cancellation of two capacitors of $-\mathbb{C}_0$ and $C_L$. We set

$$\mathbb{C}_0 = C_L. \tag{6}$$

Step 2) Selecting the characteristic impedance $\mathbb{W}_0$. We set

$$\mathbb{W}_0 = R_L. \tag{7}$$

The driving point impedance observed at the right-hand side of the transformer in Fig. 2(b) becomes $R_L$.

Step 3) Selecting the transformation ratio $k$ of the transformer. We set

$$k = \sqrt{R_L/R_0}. \tag{8}$$

The driving point impedance observed at the left-hand side of the transformer becomes the pure resistor $R_0$ of the reference impedance. The transformer ratio $k$ must be larger than unity, so that the above three steps can be carried out when the inequality

$$R_L > R_0 \tag{9}$$

is satisfied. If these procedures are completed, the driving point impedance $Z_{in}$ will become

$$Z_{in} = R_0 + \frac{1}{j\omega k C_L} \tag{10}$$

for all frequency ranges.

Step 4) Determination of network parameters of the PTL.

Equations (2)–(4) give the line length $l$, front-end characteristic impedance $W_0$, and the constant $K_1$ of the PTL as follows:

$$l = \left(R_L - \sqrt{R_0 R_L}\right) v C_L \tag{11}$$

$$W_0 = R_L/k^2 = R_0 \tag{12}$$

$$K_1 = 1/(k-1). \tag{13}$$

The line length $l$ versus $C_L$ is shown in Fig. 3 for $R_0 = 50\ \Omega$. In Fig. 3, the parameter is $R_L$, the real part of the load impedance. For higher levels of load impedance, a longer line length is needed.

*Numerical Examples:* We show these impedance transformations by numerical examples for loads of $C_L = 2$ pF and $R_L = 300$ and 500 Ω, respectively, for $R_0 = 50\ \Omega$. The parameters of the PTL are shown in Table I.

The frequency responses of the load impedance and the transformed driving point impedance are shown in Fig. 4

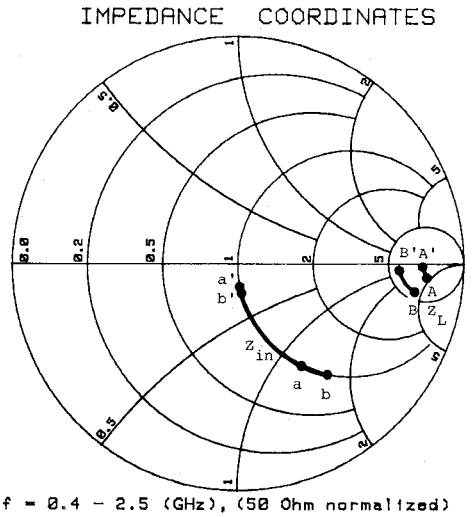


Fig. 4. The scheme of all frequency impedance transformation on the impedance chart.

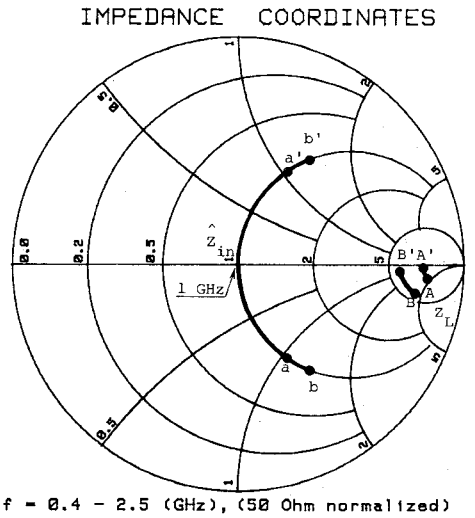


Fig. 6. The scheme of one-point impedance matching using the lumped inductor of all frequency transformation designs.

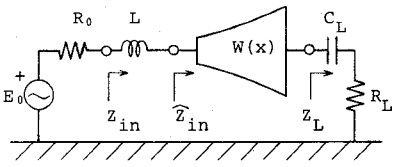


Fig. 5. The circuit diagram of achieving one-point matching using the lumped inductor.

for the frequency range $f = 0.4$–$2.5$ GHz. The impedance loci $Z_L$ of the load impedances are assigned by capital letters $A-A'$ and $B-B'$, corresponding to loads $A$ and $B$, respectively, shown in Table I, and the impedance loci $Z_{in}$ of the transformed driving point impedance are assigned by small letters $a-a'$ and $b-b'$, corresponding to loads $A$ and $B$, respectively. The load impedances whose impedance loci are located at regions of very high levels are transformed to the regions of low-impedance levels located on a unit circle of normalized resistance. Evidently, matching techniques for the transformed low-level driving point impedances are easier than those for the original load impedances.

### B. A One-Point Matching Technique

For one-point impedance matching between a generator with internal impedance $R_0$ and driving point impedance $Z_{in}$, one can use a lumped inductor $L$ in series at the front-end of the PTL by the simple technique as shown in Fig. 5. We show examples of frequency responses of the final driving point impedance $\hat{Z}_{in}$ (one-point matched) in Fig. 6 for frequency ranges of $f = 0.4$–$2.5$ GHz and the center frequency of $f_0 = 1$ GHz.

When one-point matching is carried out for these cases, the behavior of the network is that of an *RLC* series resonance circuit, so that the quality factor $Q$ of the driving point impedance $\hat{Z}_{in}$ is given by

$$Q = \frac{1}{2\pi f_0 k C_L R_0} = \frac{1}{2\pi f_0 C_L \sqrt{R_L/R_0}}. \tag{14}$$

From (14), an increase of the resistive component $R_L$ of the load impedance $Z_L$ causes a decrease of $Q$ so that the load impedances having higher resistive components give broader band frequency matching than those having lower resistive components.

### C. Impedance Transformation for Narrow Frequency Ranges

The exact impedance transformation described in Section II-A can be carried out under the inequality condition of (9). If the inequality is not satisfied, we may introduce a well-known quarter-wave matching technique for narrow-band impedance transformations. This impedance transformation is summarized in the following four steps.

Step 1) Cancellation of two capacitors of $-\mathbb{C}_0$ and $C_L$. We set

$$\mathbb{C}_0 = C_L. \tag{15}$$

Step 2) Determination of line length $l$. For a design frequency $f_0$, we set the line length $l$ of the PTL to a quarter-wavelength, i.e.,

$$l = \frac{1}{4}\frac{v}{f_0}. \tag{16}$$

In this step, the driving point impedance $Z_{in}$ becomes

$$Z_{in}(j\omega_0) = \frac{\mathbb{W}_0^2}{k^2 R_L} + \frac{1}{j\omega_0 k C_L} \tag{17}$$

at the frequency $f_0$.

Step 3) Determination of transformer ratio $k$ and characteristic impedance $\mathbb{W}_0$. If we set

$$\mathbb{W}_0 = k\sqrt{R_0 R_L} \tag{18}$$

the real part of (17) becomes $R_0$. The unknown parameter $k$ will be uniquely determined from (2)–(4), (15), and (16)

$$k = 1 + \frac{1}{4 f_0 C_L \sqrt{R_0 R_L}} > 1. \tag{19}$$

TABLE II
THE PARAMETERS OF PTL'S FOR NARROW-BAND DESIGN
($f_0 = 1$ GHz)

| $Z_L$ | | k | $W_0$ [Ω] | $K_1$ | $\ell$ [cm] |
|---|---|---|---|---|---|
| load A | $R_L$ = 500 [Ω], $C_L$ = 2 [pF] | 1.79 | 88.3 | 1.26 | 7.5 |
| load B | $R_L$ = 300 [Ω], $C_L$ = 2 [pF] | 2.02 | 60.6 | 0.980 | 7.5 |
| load C | $R_L$ = 10 [Ω], $C_L$ = 2 [pF] | 6.59 | 3.39 | 0.179 | 7.5 |

Step 4) Determination of network parameters of the PTL. The line length $l$ is given by (16), and

$$K_1 = (k-1)^{-1} = 4f_0 C_L \sqrt{R_0 R_L} \tag{20}$$

$$W_0 = \frac{\mathbb{W}_0}{k^2} = \frac{\sqrt{R_0 R_L}}{k}. \tag{21}$$

We demonstrate these narrow-band impedance transformations by numerical examples for loads $C_L = 2$ pF, and $R_L = 10$, 300, and 500 Ω for $R_0 = 50$ Ω. The parameters of the PTL are shown in Table II for a design frequency $f_0 = 1$ GHz. The frequency responses of the transformed driving point impedances $Z_{in}$ and the one-point matched driving point impedances $\hat{Z}_{in}$ (achieved by the same technique described in Section II-C) are shown in Fig. 7(a) and (b), respectively, for the frequency range $f = 0.4$–$2.5$ GHz.

## III. ADMITTANCE TRANSFORMATION AND MATCHING FOR LUMPED *RL* LOADS WITH RECIPROCAL PARABOLIC TAPERED TRANSMISSION LINES

The characteristic impedance distribution of the reciprocal parabolic tapered transmission line (RPTL) is given by

$$W'(x) = \frac{W_0}{\left(1 + \frac{1}{K_2}\frac{x}{l}\right)^2}. \tag{22}$$

An RPTL loaded by a lumped parallel $RL$ admittance $Y_L$

$$Y_L = \frac{1}{R_L} + \frac{1}{j\omega L_L} \tag{23}$$

is shown in Fig. 8(a) and its equivalent circuit is shown in Fig. 8(b) [13]. In this equivalent circuit, the circuit parameters are given as follows:

$$k = 1 + \frac{1}{K_2} > 1 \tag{24}$$

$$\mathbb{W}_0 = W_0/k^2 \tag{25}$$

$$\mathbb{L}_0 = W_0(1+K_2)l/(k^2 v). \tag{26}$$

The admittance transformation is the dual of that described in the previous section. Table III gives these formulas and information, the ratio of the imaginary to the real part of the immittance before and after the transformation, for the gain-bandwidth estimations. Fig. 9 shows the line length $l$ as a function of $L_L$ for the case of all frequency transformations.

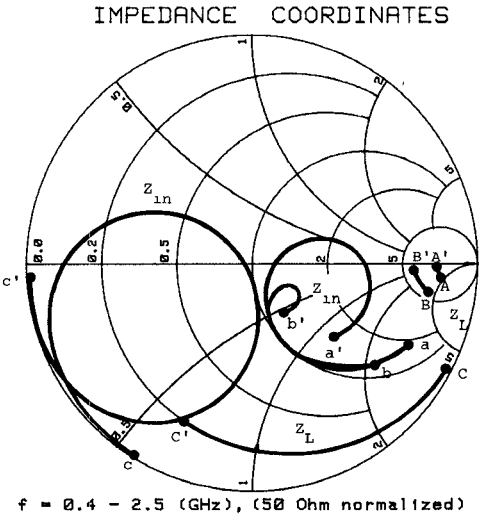


(a)

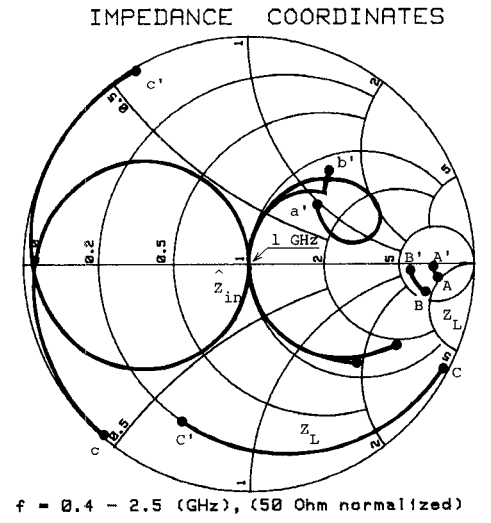


(b)

Fig. 7. The scheme of (a) narrow-band impedance transformation on the impedance chart. The impedance loci of $Z_L$ are assigned by capital letters ($A$–$A'$, $B$–$B'$, and $C$–$C'$ correspond to the load shown in Table II). The transformed impedance loci are assigned by small letters and (b) one-point impedance matching using the lumped inductor.

## IV. EXPERIMENTAL RESULTS

Two lumped series $RC$ loads and PTL's were constructed. These loads consist of a metallized film resistor and a chip capacitor in series. The measured frequency responses of these loads (load I and load II) are shown in Figs. 10 and 11, respectively, for the frequency range of 50–300 MHz, and represent good lumped impedances. In Table IV, typical values of load constants (they are determined from measured responses at $f = 150$ MHz) and parameters of the PTL's designed for all frequency transformations are listed. The line length needed for load II is very short as compared with the wavelength of the measur-

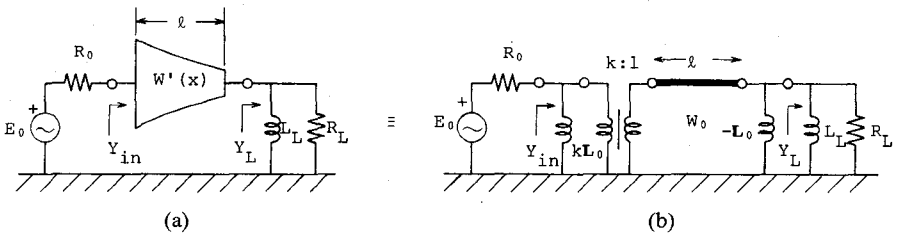


Fig. 8. (a) The reciprocal parabolic tapered transmission line loaded by the lumped parallel $RL$ admittance and (b) its equivalent circuit.

TABLE III
IMMITTANCE TRANSFORMATION FORMULAS WITH PTL AND RPTL

| | series RC impedance transformation with PTL | | parallel RL admittance transformation with RPTL | |
|---|---|---|---|---|
| | all frequency transformation | narrow frequency transformation | all frequency transformation | narrow frequency transformation |
| transmission line parameters | $\ell = (R_L - \sqrt{R_0R_L})\nu C_L$<br>$W_0 = R_0$<br>$K_1 = 1/(k-1)$<br>where<br>$k = R_L/R_0 > 1$ | $\ell = \nu/(4f_0)$<br>$W_0 = \sqrt{R_0R_L}/k$<br>$K_2 = 1/(k-1)$<br>where<br>$k = 1 + (4f_0C_L\sqrt{R_0R_L})^{-1} > 1$ | $\ell = (\frac{1}{R_L} - \frac{1}{\sqrt{R_0R_L}})\nu L_L$<br>$W_0 = R_0$<br>$K_2 = 1/(k-1)$<br>where<br>$k = R_L/R_0 < 1$ | $\ell = \nu/(4f_0)$<br>$W_0 = k\sqrt{R_0R_L}$<br>$K_2 = 1/(k-1)$<br>where<br>$k = 1 + (\sqrt{R_0R_L}/4f_0L_L) > 1$ |
| load immittance before transformation | $Z_L(j\omega) = R_L + \frac{1}{j\omega C_L}$ | $Z_L(j\omega_0) = R_L + \frac{1}{j\omega_0 C_L}$ | $Y_L(j\omega) = \frac{1}{R_L} + \frac{1}{j\omega L_L}$ | $Y_L(j\omega_0) = \frac{1}{R_L} + \frac{1}{j\omega_0 L_L}$ |
| $\left\lvert\frac{\text{(imaginary part)}}{\text{(real part)}}\right\rvert$ | $\frac{1}{\omega C_L R_L}$ | $\frac{1}{\omega_0 C_L R_L}$ | $\frac{R_L}{\omega L_L}$ | $\frac{R_L}{\omega_0 L_L}$ |
| driving point immittance after transformation | $Z_{in}(j\omega) = R_0 + \frac{1}{j\omega kC_L}$ | $Z_{in}(j\omega_0) = R_0 + \frac{1}{j\omega_0 kC_L}$ | $Y_{in}(j\omega) = \frac{1}{R_0} + \frac{1}{j\omega kL_L}$ | $Y_{in}(j\omega_0) = \frac{1}{R_0} + \frac{1}{j\omega_0 kL_L}$ |
| $\left\lvert\frac{\text{(imaginary part)}}{\text{(real part)}}\right\rvert$ | $\frac{1}{\omega kC_L R_0}$ | $\frac{1}{\omega_0 kC_L R_0}$ | $\frac{R_0}{\omega kL_L}$ | $\frac{R_0}{\omega_0 kL_L}$ |

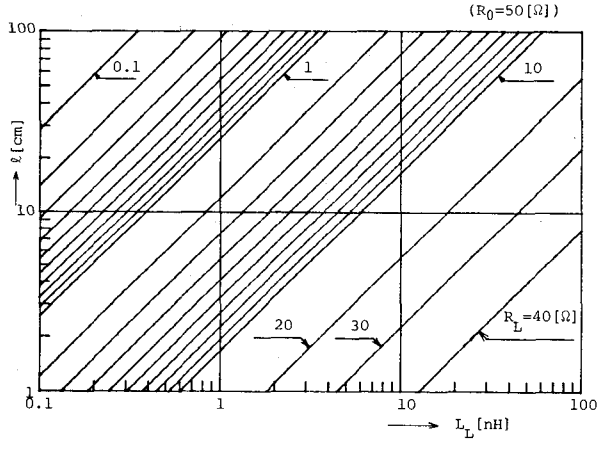


Fig. 9. The line length $l$ versus $L_L$ for $R_0 = 50\ \Omega$.

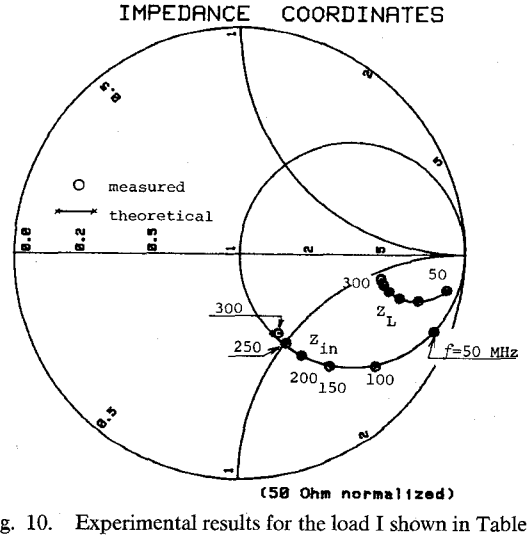


Fig. 10. Experimental results for the load I shown in Table II.

ing frequency. These PTL's are constructed in shielded microstrip.

The measured frequency responses of the driving point impedance $Z_{in}$ are shown in Figs. 10 and 11, respectively. In these figures, the theoretical responses were calculated from the load constants and PTL parameters in Table IV and the equivalent circuit shown in Fig. 2(b). Although there is a slight error apparent in the case of load II, both measured responses seem to be in good agreement with the theoretical responses. These measurements demonstrate the validity of the impedance transformation technique and the operation of the PTL notwithstanding the line length.

## V. CONCLUSIONS

We have demonstrated a simple technique for designing a parabolic tapered transmission line and reciprocal parabolic tapered transmission-line impedance transformation

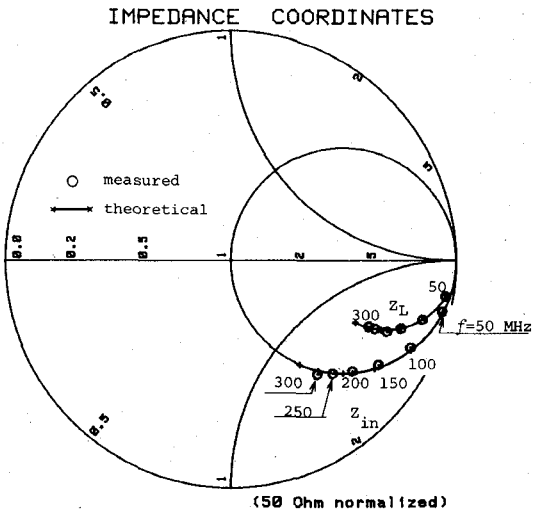


Fig. 11. Experimental results for the load II shown in Table II.

TABLE IV
TYPICAL VALUES OF LOAD CONSTANTS AND PARAMETERS OF PTL'S DESIGNED FOR ALL-FREQUENCY TRANSFORMATION

| | load constants | | parameters of PTLs | | |
|---|---|---|---|---|---|
| | $R_L$ [Ω] | $C_L$ [pF] | $W_0$ [Ω] | $K_1$ | ℓ [cm] |
| load I | 188.9 | 6.59 | 50 | 1.060 | 18.13 |
| load II | 90.2 | 3.29 | 50 | 2.913 | 2.27 |

networks for lumped *RC* and *RL* loads. Applying the parabolic tapered transmission lines, we may decrease the impedance levels of the series *RC* loads, and applying the reciprocal parabolic tapered transmission line, we may decrease the admittance levels of the parallel *RL* loads, both for all frequency ranges. Matching techniques are simpler with the use of parabolic and reciprocal parabolic tapered transmission lines as proposed in this paper. The quarter-wavelength parabolic (reciprocal parabolic) tapered transmission line can transform any lumped series *RC* (parallel *RL*) load into a convenient impedance for ordinary impedance matching in narrow frequency ranges. We have also shown experimental results for lumped *RC* loads and have demonstrated the usefulness of the parabolic and reciprocal parabolic tapered transmission lines and their equivalent circuits.

## REFERENCES


[1] G. L. Matthaei, L. Young, and E. M. T. Jones, *Microwave Filters, Impedance Matching Networks and Coupling Structures.* New York: McGraw-Hill, 1964.

[2] R. E. Collin, *Foundation for Microwave Engineering.* New York: McGraw-Hill, 1966.

[3] R. M. Fano, "Theoretical limitations on broadband matching of arbitrary impedances," *J. Franklin Inst.*, vol. 249, nos. 1 and 2, pp. 57–83, 139–154, 1950.

[4] D. C. Youla, "A new theory of broad-band matching," *IEEE Trans. Circuit Theory*, vol. CT-11, pp. 30–50, Mar. 1964.

[5] H. J. Carlin and W. Kohler, "Direct synthesis of band-pass transmission line structures," *IEEE Trans. Microwave Theory Tech.*, vol. MTT-13, pp. 283–297, May 1965.

[6] H. J. Carlin and J. J. Komiak, "A new method of broad-band equalization applied to microwave amplifiers," *IEEE Trans. Microwave Theory Tech.*, vol. MTT-27, pp. 93–99, Feb. 1979.

[7] R. Levy and J. Helszajn, "Specific equation for one and two section quarter-wave matching networks for stub-resistor loads," *IEEE Trans. Microwave Theory Tech.*, vol. MTT-30, pp. 55–63, Jan. 1982.

[8] A. T. Starr, "The nonuniform transmission line," *Proc. IRE*, vol. 20, pp. 1052–1063, June 1932.

[9] H. Kaufman, "Bibliography of nonuniform transmission lines," *IRE Trans. Antennas Propagat.*, vol. AP-3, pp. 218–220, Oct. 1955.

[10] M. N. S. Swamy and B. B. Bhattacharyya, "Hermite lines," *Proc. IEEE*, vol. 54, pp. 1577–1578, Nov. 1966.

[11] B. S. Westcott, "Generalized confluent hypergeometric and hypergeometric transmission lines," *IEEE Trans. Circuit Theory*, vol. CT-16, pp. 289–294, Aug. 1969.

[12] M. J. Ahmed, "Impedance transformation equation for exponential, cosine-squared, and parabolic tapered transmission lines," *IEEE Trans. Microwave Theory Tech.*, vol. MTT-29, pp. 67–68, Jan. 1981.

[13] K. Kobayashi, Y. Nemoto, and R. Sato, "Kuroda's identity for mixed lumped and distributed circuits and their application to nonuniform transmission lines," *IEEE Trans. Microwave Theory Tech.*, vol. MTT-29, pp. 81–86, Feb. 1981.

[14] K. Kobayashi, Y. Nemoto, and R. Sato, "Equivalent representations of nonuniform transmission lines based on the extended Kuroda's identity," *IEEE Trans. Microwave Theory Tech.*, vol. MTT-30, pp. 140–146, Feb. 1982.


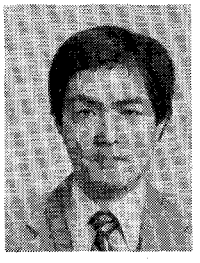

**Isao Endo** was born in Fukushima, Japan, on August 17, 1949. He received the B.E. and M.E. degrees in electronics engineering from Ibaraki University, Hitachi, Japan, in 1973 and 1975, respectively.

From 1975 to 1980, he was a Research Associate and, from 1980 to 1983, he was a Lecturer in the Department of Electric Engineering, Ibaraki Technical College, Katsuta, Japan. He is now an Associate Professor. His research interests include circuit theory and matching network design.

Mr. Endo is a member of the Institute of Electronics and Communication Engineers of Japan.

**Yoshiaki Nemoto** (S'72–M'73) was born in Sendai City, Miyagiken, Japan, on December 2, 1945. He received the B.E., M.E., and Ph.D. degrees from Tohoku University, Sendai, Japan, in 1968, 1970, and 1973, respectively.

Since 1973, he has been a Research Associate with the Faculty of Engineering, Tohoku University. He has been engaged in research works in distributed networks and computer networks using satellites. He is co-recipient of the 1982 Microwave Prize from the IEEE Microwave Theory and Techniques Society.

Dr. Nemoto is a member of the Institute of Electronics and Communication Engineers of Japan.

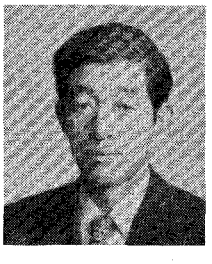

**Risaburo Sato** (SM'62–F'77) was born in Furukawa City, Miyagiken, Japan, on September 23, 1921. He received the B.E. and the Ph.D. degrees from Tohoku University, Sendai, Japan, in 1944 and 1952, respectively.

From 1949 to 1961, he was an Assistant Professor at Tohoku University, and in 1961 he became a Professor in the Department of Electrical Communications at the same university. Since 1973, he has been a Professor in the Department of Information Science at Tohoku University. From 1969 to 1970, he was an International Research Fellow at Stanford Research Institute, Menlo Park, CA. His research activities include stud-

ies of multiconductor transmission systems, distributed transmission circuits, antennas, communication systems, active transmission lines, magnetic and ferroelectric recording, neural information processing, computer networks, and electromagnetic compatibility. He has published a number of technical papers and some books in these fields, including *Transmission Circuit*. He received the Paper Award from the Institute of Electrical Engineers of Japan (IEE of Japan) in 1955, the Kahoku Press Cultural Award in 1963, an award from the Invention Association of Japan in 1966, the Paper Award from the Institute of Electronics and Communication Engineers of Japan (IECE of Japan) in 1980, a Certificate of Appreciation of Electromagnetic Compatibility from the IEEE in 1981, and the Microwave Prize of the Microwave Theory and Techniques Society of IEEE in 1982.

Dr. Sato was the Vice President of IECE of Japan from 1974 to 1976. He has been a member of the Science Council of Japan from 1978 and a member of the Telecommunication Technology Consultative Committee at NTT from 1976. He is a chairman of EMC-S Tokyo Chapter of IEEE and a member of B.O.D. of EMC-S of IEEE. He is also a member of IECE of Japan, IEE of Japan, the Institute of Television Engineers of Japan, and the Information Processing Society of Japan.

# Lossy Inductive-Post Obstacles in Lossy Waveguide

PING GUAN LI AND ARLON TAYLOR ADAMS, SENIOR MEMBER, IEEE

*Abstract*—**Post and wall losses are treated for inductive obstacles in rectangular waveguide. Post losses are treated rigorously by moment methods and wall losses are obtained by perturbational methods. Losses may be taken into account by a modified equivalent circuit and a lossy transmission line. Post losses may be comparable to wall losses.**

## I. Introduction

INDUCTIVE POSTS in rectangular waveguide have been treated by many researchers [1]–[7], starting with the classical treatment by Schwinger. A recent analysis [8] by the authors utilized a Galerkin moment-method solution. The post currents are represented in terms of a Fourier series $\sum_{-\infty}^{\infty} A_n e^{jn\phi}$ and as many terms of the series as necessary are used, enabling one to treat arbitrary post configurations. The extension to lossy posts and lossy walls is considered in this paper. Post losses are treated rigorously by moment methods in a direct extension of the analysis of [8]. The post losses are taken into account by a modification of the equivalent circuit of the obstacle; resistive elements are added and reactive elements are changed in value. The wall losses are obtained by perturbational methods. Orthogonality is not maintained for wall losses. The waveguide is separated in several regions (with different numerical methods applicable to each) and the total wall losses are calculated. The wall losses may then be separated into two parts: a) the total minus dominant mode (or excess) wall losses, and b) the dominant mode wall losses. The latter may be treated by a lossy transmission-line model and the former may be treated by further modification of the lumped equivalent circuit. Typical results are presented. It is noted that post losses are significant and may in some cases be comparable to wall losses.

Manuscript received March 2, 1984; revised July 30, 1984.

The authors are with the Department of Electrical and Computer Engineering, Syracuse University, Syracuse, NY 13210

For efficient analysis of post filters, the cascading of equivalent circuits (i.e., the neglect of higher order mode interactions) is desirable. It has been shown in [8] that such an assumption is reasonable, even for high-$Q$ filters. The treatment described above permits such a cascaded model for lossy filter analysis.

## II. Post Losses

Fig. 1 shows a lossy cylindrical inductive post in a rectangular waveguide. A dominant mode traveling in the $z$ direction is incident upon the post. A cylindrical coordinate system is centered on the post axis at $z = 0$, $y = c$. The incident electric field may be expressed as

$$E_x^i = E_o e^{-jk'z} \sin \frac{\pi y}{a} \tag{1}$$

where

$$k' = \sqrt{k^2 - \left(\frac{\pi}{a}\right)^2} = \frac{2\pi}{\lambda_g}, \quad \text{and } k = \frac{2\pi}{\lambda}.$$

The incident electric field can also be expressed in the Fourier-series form [8]

$$E_x^i = \sum_{n=-\infty}^{\infty} (-1)^n E_o \sin\left(\frac{\pi c}{a} - n\alpha\right) J_n(kr) e^{jn\theta} \tag{2}$$

where

$$\alpha = \tan^{-1}\left(\frac{\pi}{k'a}\right).$$

The induced volume current density inside the post may be represented as

$$J_x(r,\theta) = \sum_{n=-\infty}^{\infty} a_n' \frac{J_n(k_c r)}{J_n(k_c r_o)} e^{jn\theta} \tag{3}$$

where $k_c$ is the wavenumber of the conductor. For a good

0018-9480/85/0100-0008$01.00 ©1984 IEEE